A Novel Nude Mouse Model of Hypertrophic Scarring Using Scratched Full Thickness Human Skin Grafts

Saad M. Alrobaiea,[1] Jie Ding,[1] Zengshuan Ma,[1] and Edward E. Tredget[1,2,*]

[1]Wound Healing Research Group, Department of Surgery, University of Alberta, Edmonton, Canada.
[2]Divisions of Plastic and Reconstructive Surgery and Critical Care, University of Alberta, Edmonton, Canada.

Objective: Hypertrophic scar (HTS) is a dermal form of fibroproliferative disorder that develops following deep skin injury. HTS can cause deformities, functional disabilities, and aesthetic disfigurements. The pathophysiology of HTS is not understood due to, in part, the lack of an ideal animal model. We hypothesize that human skin with deep dermal wounds grafted onto athymic nude mice will develop a scar similar to HTS. Our aim is to develop a representative animal model of human HTS.

Approach: Thirty-six nude mice were grafted with full thickness human skin with deep dermal scratch wound before or 2 weeks after grafting or without scratch. The scratch on the human skin grafts was made using a specially designed jig that creates a wound >0.6 mm in depth. The xenografts were morphologically analyzed by digital photography. Mice were euthanized at 1, 2, and 3 months postoperatively for histology and immunohistochemistry analysis.

Results: The mice developed raised and firm scars in the scratched xenografts with more contraction, increased infiltration of macrophage, and myofibroblasts compared to the xenografts without deep dermal scratch wound. Scar thickness and collagen bundle orientation and morphology resembled HTS. The fibrotic scars in the wounded human skin were morphologically and histologically similar to HTS, and human skin epithelial cells persisted in the remodeling tissues for 1 year postengraftment.

Innovation and Conclusions: Deep dermal injury in human skin retains its profibrotic nature after transplantation, affording a novel model for the assessment of therapies for the treatment of human fibroproliferative disorders of the skin.

Edward E. Tredget, MD, MSc

Submitted for publication July 30, 2015. Accepted in revised form September 8, 2015.

*Correspondence: Wound Healing Research Group, Department of Surgery, University of Alberta, 2D2.31 Walter Mackenzie Center, 8440-112 Street, Edmonton T6G 2B7, Alberta, Canada (e-mail: etredget@ualberta.ca).

INTRODUCTION

Skin wound healing is an extremely complex process that involves the reactions and interactions of inflammatory cells, growth factors, and cytokines.[1] This orchestrated process can be divided into four overlapped phases starting with hemostasis, followed by inflammation and proliferation, and ending by maturation, including collagen remodeling to restore the damaged skin integrity through formation of a mature scar.[1–3]

Hypertrophic scar (HTS) is a dermal form of fibroproliferative disease (FPD) that develops after burns and deep skin injuries or even planned surgical wounds.[4] It presents as a hyperemic, elevated firm scar not exceeding the boundaries of the original site of injury.[5] These scars often cause contracture deformities leading to permanent disabilities, aesthetic disfigurement, and prolonged period of hospitalization and rehabilitation.[6] Increased cell

DOI: 10.1089/wound.2015.0670

proliferation, excess blood vessel formation, collagen deposition, and thin disorganized collagen fibers in the dermis in addition to the presence of α-smooth muscle actin (α-SMA)–expressing cells are the main histological features of HTS. Imbalance in the synthesis and degradation of extracellular matrix (ECM) components by fibroblast leads to the development of dermal fibrosis typical of HTS.[7]

Despite many proposed treatments to date, there are still few, if any, reliable efficient forms of therapy for HTS. In addition, the current treatments of HTS require prolonged periods to be effective and tend to be expensive with considerable side effects.[8,9] One major investigative hurdle in dermal FPD is the lack of an ideal animal model, which responds to injury similar to humans.[10,11]

Dunkin *et al.* have described a progressively deep dermal injury in the lateral thigh skin of 113 human volunteers, which heals without scar in the superficial regions of the wound.[12] However, in the deeper regions of the progressively deep injury, a red raised HTS develops when the wounds exceed 0.56 mm in depth. Honardoust confirmed these findings and described increased transforming growth factor-β (TGF-β), large molecular weight proteoglycans, and less decorin and type II TGF-β receptors in the deeper tissues typical of immature human HTS.[13] Fibroblasts from these deeper layers of the skin have been found to possess many or most features of the HTS fibroblasts compared to superficial dermal fibroblasts and site-matched normal skin fibroblasts. In contrast, considerable evidence supports the importance of bone marrow-derived monocytes and fibrocytes in the development of HTS.[14] However, it is unclear on the relative importance of resident fibroblasts in the deep dermis of the skin versus infiltrating immune cells in the development of HTS and their persistence in the remodeling scar over time.

CLINICAL PROBLEM ADDRESSED

Unfortunately, few representative animal models of HTS exist currently, and many investigators have questioned the value of therapies developed and tested in rabbits and pigs, which do not appear to translate into effective therapies for dermal fibrosis in humans.[15,16] Thus, by creating wounds in human skin, which are known to reliably develop HTS, and transplanting the skin to athymic mice, we seek to answer questions about the quantitative importance of deep dermal fibroblasts resident in human skin and to clearly identify bone marrow-derived cells in the fibrotic tissues and their role in the developing scar. Thus, it is our goal to develop this model to improve our understanding of dermal fibrosis and allow for the development of novel and safe antifibrotic treatments that will reliably translate into effective therapies for fibrotic disorders in human skin.[17]

MATERIALS AND METHODS

Preparation of skin grafts

Full thickness human skin samples were obtained from female patients who underwent elective abdominoplasty procedure following informed written consent. Full thickness skin grafts were obtained from the lower abdominal skin, avoiding the damaged areas that contained stretch marks. Excessive subcutaneous fat was removed manually with curved iris scissors before cutting it into 3.0×1.5 cm grafts with a scalpel. Thereafter, a scratch wound was made on each graft using a No. 11 scalpel blade in a specially designed modification of a jig originally described by Dunkin *et al.*[12] as illustrated in Fig. 1. The modified jig creates a 2 cm long wound that is >0.6 mm deep in each of the grafts. Thereafter, the grafts were stored in sterile normal saline at 4°C until the time of grafting.

Transplantation of skin grafts

All animal experiments were performed using protocols approved by the University of Alberta Animal Care and Use Committee meeting the standards of the Canadian Council on Animal Care. The mice were housed in a virus antibody-free biocontainment facility for the entire experiment and conditioned for 2 weeks before experimentation.

Thirty-six male athymic nude mice at 4 weeks of age weighing ~25 g were purchased from Charles River Laboratories International, Inc. (Wilmington, MA). The animals were divided into the following three groups: mice grafted with human skin without scratch wound, mice grafted with human

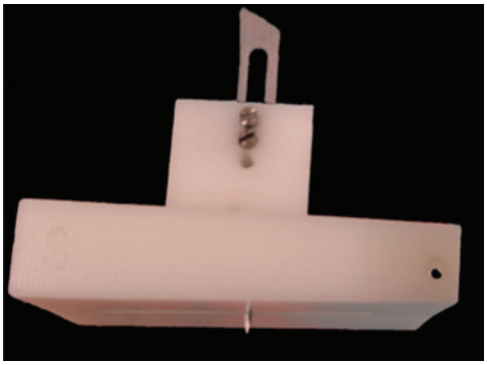

Figure 1. The jigsaw used to make scratch wound on human skin grafts. To see this illustration in color, the reader is referred to the web version of this article at www.liebertpub.com/wound

skin with scratch wound before grafting, and mice that were anesthetized before performing the scratch procedure in the engrafted human skin at 2 weeks after transplantation. Within each group, the mice were euthanized at 1, 2, and 3 months after grafting and there were four mice in each time point and each experimental group.

In the prone position under isoflurane anesthetic (Halocarbon Laboratories, River Edge, NJ), the dorsal skin surface was disinfected with iodine. A 3.0×1.5 cm skin area was marked using a prefabricated plastic template as previously described.[18] The full thickness skin was excised using surgical scissors, leaving the panniculus carnosus intact. Then, full thickness human skin grafts with or without scratch wound were transplanted and sutured with 4-0 silk suture (Ethicon, Somerville, NJ) using a tie-over bolus dressing technique with a nonadherent petrolatum (Xeroform™; Covidien, Mansfield, MA) and dry gauze to ensure adherence of the graft to the wound bed as previously described.[18–20] All animals received narcotic analgesia (Hydromorphone HP 10 diluted to 0.05 mg/mL; Sandoz, Boucherville, QC) subcutaneously for pain management following grafting. The dressing and the stitches were removed 2 weeks after the surgery. At this time, a scratch wound was made in the xenografted human skin tissue in four mice using the previously described jig for each of the three time points. The graft morphology was monitored weekly by digital photography using standardized conditions, in which the distance from the animal, lighting, and exposure was constant. Animals were euthanized at 1, 2, and 3 months postgrafting to harvest the human skin xenografts for histology and immunohistochemistry analysis.

In a separate experiment, two athymic nude mice were grafted with skin samples from an African American female patient who underwent an elective abdominoplasty. Scratch wounds using the above-mentioned technique were made before grafting onto the back of nude mice to clinically observe the persistence of the dark melanin containing keratinocytes and dermal elements of the scratched grafts for 1 year after transplantation.

Histologic analysis of human skin xenografts

Biopsies were harvested from xenografts' unscratched skin or skin xenografts with scratch wound before or after transplantation at all three time points. Each was divided into two parts. The first part was fixed in 10% formalin (Zinc Formal-Fixx™; Thermo Scientific, Pittsburgh, PA) for 24 h, processed, and embedded in paraffin. These blocks were cut to 5 μm sections, mounted on glass slides, and subjected to hematoxylin and eosin (H&E), Masson's trichrome, α-SMA, toluidine blue, and picrosirius red staining. The second part was embedded and frozen in CryoMatrix (Shandon Cryomatrix™; Thermo Scientific). The frozen blocks were cut into 10 μm sections and mounted on glass slides that were used for macrophage and human leukocyte antigen (HLA)-ABC staining.

Measurements of the wound area

As described previously[20] using the weekly photographs taken with a ruler in standardized conditions to document wound healing and scar formation, ImageJ software (National Institutes of Health, Bethesda, MD) was used to measure the graft area in the photos to assess the wound area over time.

Histological analysis of graft thickness

Graft thickness was evaluated in H&E staining viewed under 100× magnification using bright field microscopy. The distance from the stratum corneum to the dermal–fat junction was measured using ImageJ software (National Institutes of Health) in five random high-power fields in sections from each time point. Graft thickness measurement is expressed as the mean fold change by calculating the ratio of the graft thickness (final value) to the normal human skin thickness before grafting (initial value).

Immunohistochemical analysis of macrophages

As previously reported,[19] frozen sections were warmed at room temperature for 30 min, fixed in ice-cold acetone for 5 min, then air-dried for 10 min. After blocking with 10% bovine serum albumin (BSA; Sigma-Aldrich, Inc., St. Louis, MO) for 1 h, the endogenous peroxidase activity was quenched with 3% hydrogen peroxide. Sections were incubated with primary antibodies of rat anti-mouse F4/80 (eBioscience, San Diego, CA) at 1:100 dilution in 1% BSA overnight at 4°C. Thereafter, the secondary antibody, biotinylated rabbit anti-rat immunoglobulin G (IgG; Dako, Glostrup, Denmark), was applied at 1:500 dilution in 1% BSA for 30 min at room temperature. Secondary detection was done after incubation with VECTASTAIN® Elite avidin–biotin complex (ABC reagent) for 30 min and washing the slides with peroxidase substrate and 3, 3′-diaminobenzidine (DAB; Vector Laboratories, Inc., Burlingame, CA). Finally, counterstaining was performed using hematoxylin and the sections were dehydrated through five changes of increasing concentrations of ethanol before mounting the slides with permount (Fisher Scientific Company, Fair

Lawn, NJ) and covering with glass coverslips. For negative controls, staining with the primary antibody was replaced with 1% BSA. F4/80-positive macrophages were counted in five random HPFs under ×200 magnification in all sections. Macrophage numbers are expressed as the mean fold change by calculating the ratio of number of macrophages in the grafts (final value) to the number of macrophages in normal mouse skin before grafting (initial value).

Immunohistochemical staining for α-SMA–expressing myofibroblasts

Paraffin-embedded human xenograft sections were used to stain for α-SMA as previously reported.[18,20] Sections were deparaffinized and rehydrated in five decreasing gradients of ethanol and then treated for antigen retrieval with 0.05% trypsin before blocking with 10% BSA for 1 h. Thereafter, sections were incubated with primary antibody of rabbit anti-αSMA (Millipore, Billerica, MA) and 1:1,000 dilution in 1% BSA overnight at 4°C. The secondary antibody of goat anti-rabbit IgG (Dako) was applied at 1:500 dilution in 1% BSA for 30 min at room temperature. The Vectastain Elite ABC Kit (Vector Laboratories, Inc.) was applied for 30 min and washed with peroxidase substrate DAB (Vector Laboratories, Inc.) before counterstaining with hematoxylin. Dehydration through five changes of increasing gradient ethanol was made before mounting the slides with permount (Fisher Scientific Company) and glass coverslips. Staining with primary antibody was omitted for staining control resulting in negative staining. Brown positively stained cells were counted in five random HPFs under ×200 magnification in all sections. α-SMA–expressing myofibroblast numbers are expressed as the mean fold change by calculating the ratio of the cell number in the grafts (final value) to the cell number in normal human skin before grafting (initial value).

Toluidine blue staining for mast cells

Toluidine blue staining was used to detect mast cells as previously described.[18,19] Paraffin sections were deparaffinized and rehydrated through five changes of decreasing gradient ethanol. Sections were then incubated with toluidine blue (Toluidine Blue O; Fisher Scientific Company) solution for 2 to 3 min, followed by washing in distilled water. Finally, sections underwent dehydration by five changes of increasing gradient ethanol before clearing them with two changes of xylene and mounting with permount (Fisher Scientific Company) and glass coverslips. Positively stained red-purple mast cells were quantified in five random HPFs in all sections. Mast cell numbers are expressed as the mean fold change by calculating the ratio of the cell number in the grafts (final value) to the cell number in normal human skin before grafting (initial value).

Masson's trichrome staining for collagen bundle

Masson's trichrome staining was used to detect collagen bundles in the dermis. Paraffin-embedded sections of human HTS, human normal skin, and skin graft biopsies from mice were deparaffinized and rehydrated before staining in Weigert's iron hematoxylin, Biebrich scarlet acid, and phosphomolybdic–phosphotungstic acid for 10 min each. The sections were then transferred directly to aniline blue and stained for 10 min further. After rinsing in distilled water and differentiating in 1% acetic acid for 5 min, the sections were dehydrated and mounted. Collagen fibers were visualized in green, nuclei in black, and keratin in red under the bright field microscope.

Picrosirius red staining for collagen orientation

Using paraffin-embedded sections as previously described,[18,21] picrosirius red staining was used to assess the birefringence of the collagen fibers of human HTS, human normal skin, and human xenograft biopsies from mice. Briefly, sections were deparaffinized and rehydrated through five changes of decreasing gradient ethanol before incubating them in Sirius red (Sigma-Aldrich, Inc.) and picric acid (Sigma-Aldrich, Inc.) solution for 1 h at room temperature. Thereafter, sections were washed in two changes of acidified water, dehydrated in 100% ethanol, and cleared in xylene. The slides were then mounted with permount (Fisher Scientific Company) and covered with glass coverslips, then examined using a polarizing microscope (Axio Imager. A1; Carl Ziess MicroImaging, Inc., Thornwood, NY).

Human HLA-ABC staining for evaluation of human skin survival in the mouse body

To assess the human skin survival as previously reported,[18] frozen sections were warmed at room temperature for 30 min, fixed in ice-cold acetone for 5 min, then air-dried for 10 min. After blocking with 10% BSA, sections were incubated overnight at 4°C with FITC-labeled anti-human HLA-ABC antibody (Accurate Chemical & Scientific Corp., Westbury, NY) diluted to 1:50 in 1% BSA. Samples were washed with Tris-buffered saline before mounting. The mounted slides were stained with the ProLong Gold antifade reagent with DAPI (Life Technologies, Carlsbad, CA), sealed with coverslips, and examined with the fluorescence microscopy Zeiss

AxioImager M2 instrument (Jena, Germany). The primary antibody was omitted resulting in negative staining.

Statistical analysis

Four mice for each time point and each group were used. Statistical analysis was performed using analysis of variance with Tukey multiple comparison in Prism 6 for Mac (GraphPad Software, Inc.). Data are expressed as mean ± standard error, with significance set at p-value ≤0.05

RESULTS

Morphological observations

The transplanted human skin grafts were clinically viable throughout the experiment. After removing the dressing from the mice, the xenografts were soft and pink and the scratch area started to heal. At 2 weeks, the scratch area was completely closed and the whole xenograft had started to become elevated and hardened compared to the surrounding mouse skin. Furthermore, at 2 months after the procedure, the xenografts started turning red, raised, and indurated more than the normal mouse skin. These features persisted to the end of the study showing features of HTS, and the scratched area over the grafts healed similar to adjacent grafted human skin. Nevertheless, the scratch wound grafts, whether before or after grafting, contracted more than the nonscratch wound grafts (Fig. 2). The two scratched xenografts from an African American skin sample healed in the same manner, and the scratched wounds healed with same color of the adjacent human skin and were viable for 1 year after grafting (Fig. 3). This showed a morphological evidence of human cell viability and the contribution in the development of the fibrotic xenografts.

The total wound area of engrafted tissues as quantitated and displayed in Fig. 4 suggested that the wound area of the grafts continued to contract in all the groups over time. There was no significant difference between the three groups at the first month post-transplantation. However, the scratch wounds before and after grafting resulted in more graft contraction compared to the nonscratched skin grafts at 2 months post-transplantation (1.83 ± 0.073 and $1.88 \pm 0.054\,cm^2$ vs. $2.51 \pm 0.011\,cm^2$, respectively $p < 0.05$) and at 3 months post-transplantation (1.68 ± 0.076 and $1.63 \pm 0.15\,cm^2$ vs. $2.12 \pm 0.07\,cm^2$, respectively $p < 0.05$).

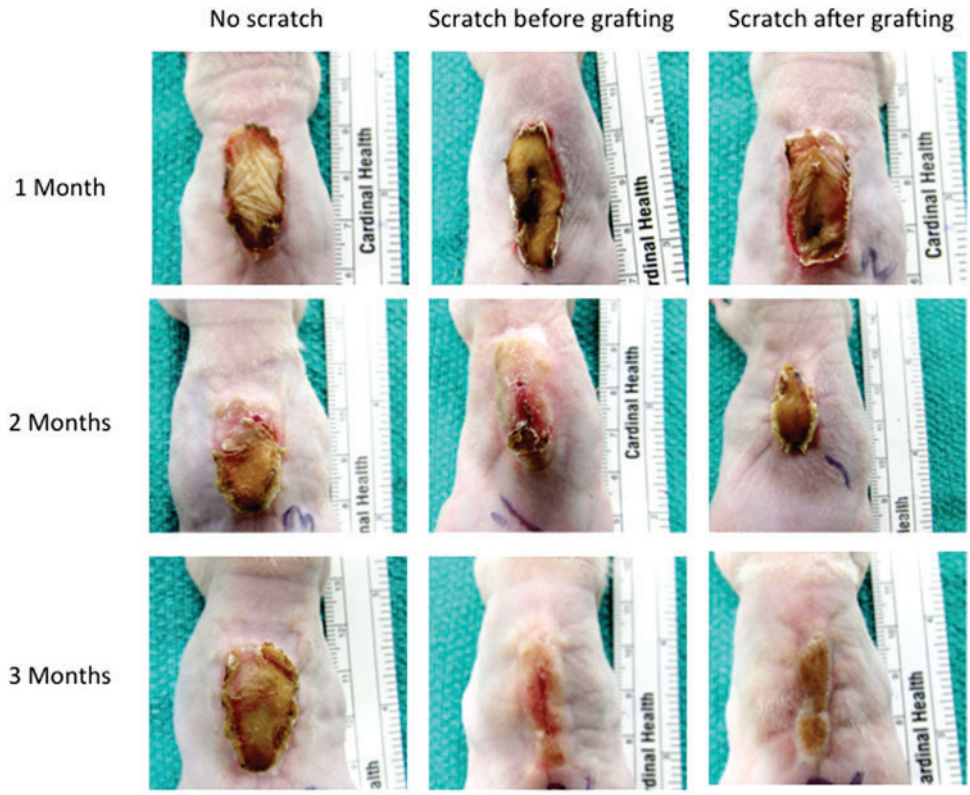

Figure 2. Morphological observation of the graft development over time showing the *red* elevated grafts compared to the mouse skin. The scratch in the grafts made wound contract more than the ones without scratch. To see this illustration in color, the reader is referred to the web version of this article at www.liebertpub.com/wound

Figure 3. The graft survived, and the scratch in it healed preserving the color of the human skin for 1 year after grafting. To see this illustration in color, the reader is referred to the web version of this article at www.liebertpub.com/wound

Scratched grafts developed similar histologic characteristics of HTS

Quantification of xenografted human skin tissue showed a gradual increase in xenograft thickness of all the groups over time. The thickness of xenografts from mice grafted with the scratched human skin performed either before or after grafting peaked at 2 months and then decreased, while the nonscratched xenografts continued to show a steady increase in thickness (Fig. 5). The skin grafts in the deep dermal scratch performed before and after grafting the mice were thicker at 2 months compared to the intact nonscratched grafts (2.15 ± 0.15 and 2.27 ± 0.1 vs. 1.3 ± 0.12 mean fold change, respectively $p < 0.05$) postengraftment. Nevertheless, the presence of a deep dermal injury in the skin grafts, whether performed either before or after grafting, resulted in no significant difference in dermal thickness and fibrosis compared to intact nonscratched grafts at 1 and 3 months postengraftment.

Dermal collagen organization and accumulation were assessed using Masson's Trichrome stain in xenografts from all time points (Fig. 6), which demonstrated that the normal basket-weave pattern of the collagen fibers seen in normal human skin was replaced with thin collagen fibers that were oriented parallel to the skin surface in all the grafts, which is similar to human HTS. Using picrosirius red staining and polarized light microscopy, collagen fibers in the human skin grafts appeared thin with yellow-orange birefringence similar to human HTS in contrast to the collagen fibers in the normal human skin, which are thicker with a basket-weave morphology (Fig. 7).

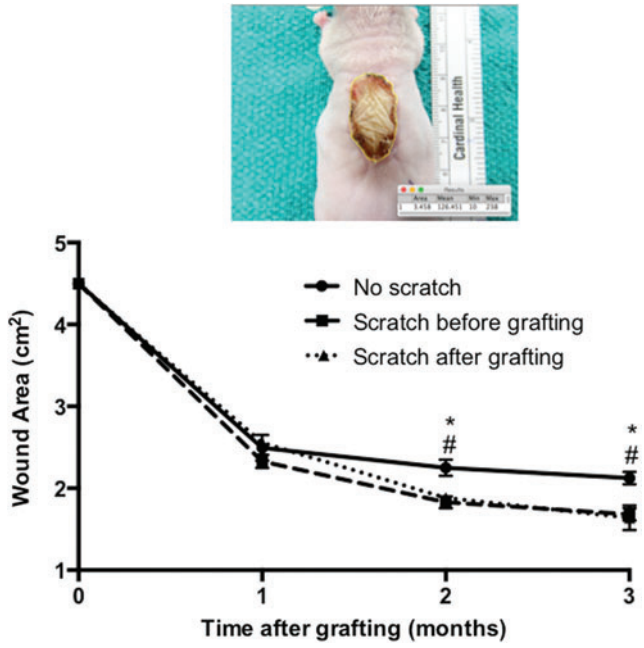

Figure 4. Representative image of the wound area and the quantification of the wound areas over time after grafting measured using ImageJ software. No scratch grafts (*circle*), scratch before grafting (*square*), and scratch after grafting (*triangle*). $^{\#}p < 0.05$ compared between the scratch before grafting and no scratch group in the same time point. $^{*}p < 0.05$ compared between the scratch after grafting and no scratch group in the same time ($n = 4$). To see this illustration in color, the reader is referred to the web version of this article at www.liebertpub.com/wound

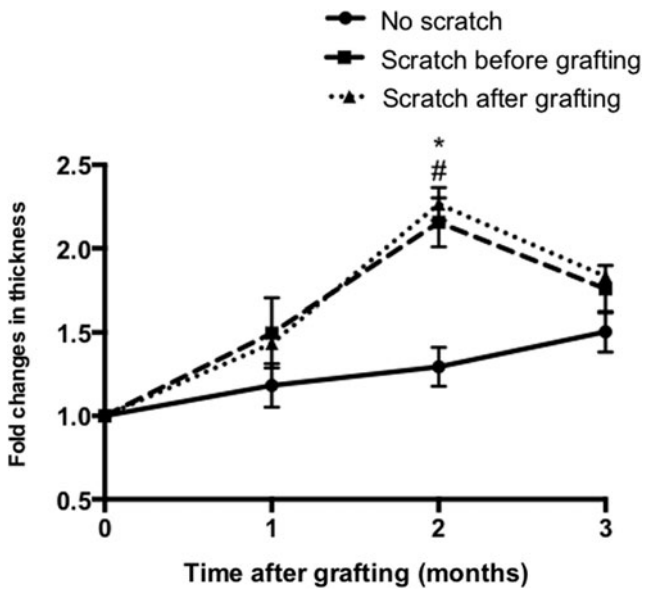

Figure 5. Fold changes in dermal thickness of the grafted skin, the distance was measured from the stratum corneum to the dermal–fat junction in five randomly selected sites/field. No scratch grafts (*circle*), scratch before grafting (*square*), and scratch after grafting (*triangle*). $^{\#}p < 0.05$ compared between the scratch before grafting and no scratch group at the same time point. $^{*}p < 0.05$ compared between the scratch after grafting and no scratch group at the same time ($n = 4$).

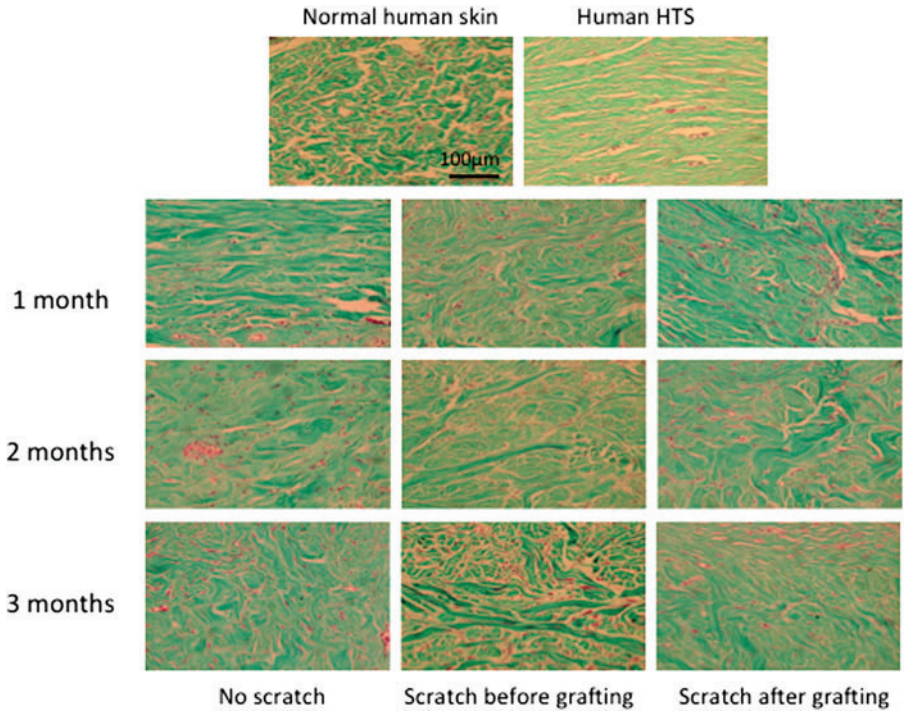

Figure 6. Representative images of Masson's trichrome staining tissue sections of human normal skin, human hypertrophic scar (HTS), and xenografts from all time points. Showing basket-weave collagen bundle in normal skin in contrast to the whorled collagen bundle of xenografts that are consistent with HTS. Scale bar = 100 μm. To see this illustration in color, the reader is referred to the web version of this article at www.liebertpub.com/wound

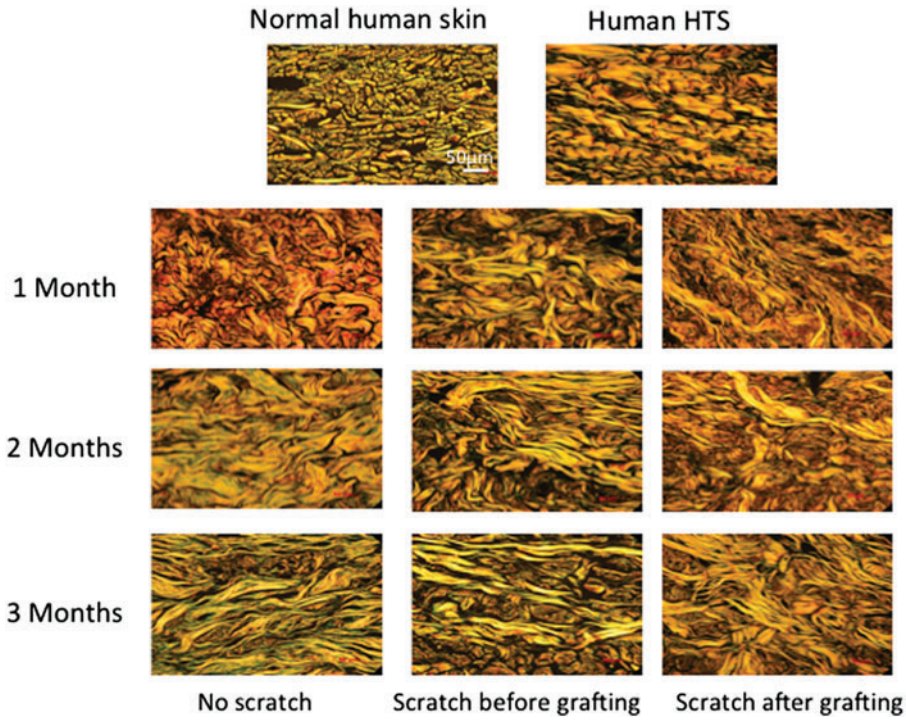

Figure 7. Representative images of a picrosirius red stained section of human normal skin, human HTS, and xenografts from all time points. Showing randomly oriented, thick with basket weave pattern collagen fiber in normal human skin compared to the thin fibers that are oriented parallel to the skin surface of the xenografts similar to HTS. Scale bar = 50 μm. To see this illustration in color, the reader is referred to the web version of this article at www.liebertpub.com/wound

Scratching the grafts increase α-SMA–expressing myofibroblast formation

Immunohistochemistry staining for α-SMA detected and quantified myofibroblast formation in xenografts at all time points (Fig. 8A). A high density of spindle-shaped cells was present in the xenografts at each time point, similar to human HTS but different from normal human skin, where the α-SMA–expressing cells appeared to be vascular smooth muscle cells associated with the endothelium.[8] Quantification of the numbers of the α-SMA–expressing cells in the scratch wounds before or after grafting, respectively, demonstrated significantly increased α-SMA–expressing cells at 2 months compared to nonscratched wound xenografts (3.64 ± 0.16 and 3.52 ± 0.24 vs. 2.4 ± 0.23 mean fold change, respectively $p < 0.05$), which may be related to the higher contractility of the skin grafts seen in the scratch wound grafts, which was significantly different at the peak of contraction at 2 months post-transplantation. Furthermore, the scratch after grafting xenografts showed more α-SMA–expressing cells than nonscratched xenografts at 3 months post-transplantation (2.12 ± 0.19

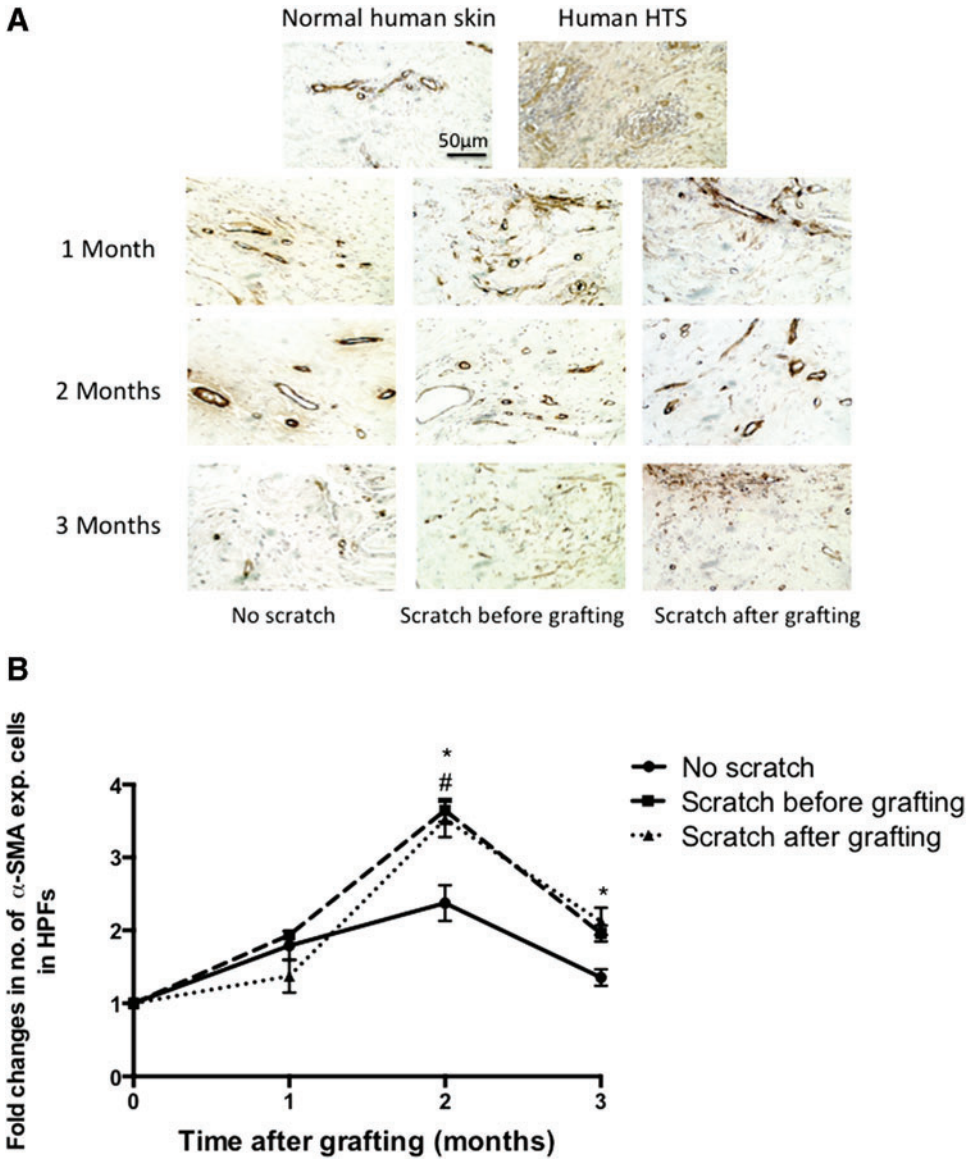

Figure 8. **(A)** Representative image of an α-smooth muscle actin (α-SMA) stained section of human normal skin, HTS, and transplanted xenografts at all time points showing a positive brown staining, indicating the presence of myofibroblasts throughout the dermis consistent with HTS. Normal human dermis stains positive only around blood vessels. Scale bar = 50 μm. **(B)** Fold changes in α-SMA–expressing cells, measured in five randomly selected site/field. No scratch grafts (*circle*), scratch before grafting (*square*), and scratch after grafting (*triangle*). $^{\#}p < 0.05$ compared between the scratch before grafting and no scratch group in the same time point. $^{*}p < 0.05$ compared between the scratch after grafting and no scratch group in the same time ($n = 4$). To see this illustration in color, the reader is referred to the web version of this article at www.liebertpub.com/wound

vs. 1.35 ± 0.11 mean fold change, $p = 0.014$) and there was no significant difference between the scratched before group (2.0 ± 0.11) and nonscratch group at 3 months (Fig. 8B).

Retention of human skin cells post-transplantation

Staining for HLA-ABC was used for the detection of the surviving of human cells in the skin grafts on the back of the mice where HLA-ABC antigens were used to detect nucleated human cells. Using direct immunofluorescent staining for HLA-ABC in skin grafted tissues at all time points, retention of green staining patterns in the epidermal and dermal cells of the grafts was similar to the staining seen in fresh human skin compared to the negative control mouse skin where little or no staining was present. This confirms the retention of viable human cellular elements in the tissues engrafted for several months post-transplantation even in the grafts, which sustained the deep dermal scratch performed before or at 2 weeks post-transplantation (Fig. 9) rather than a gradual replacement of human cells in the skin grafts with mouse cells infiltrating from the wound bed.

Scratch wounds increase macrophage infiltration in human xenografts

Immunohistochemistry staining for F4/80 was used to detect macrophages in all tissue sections from all time points (Fig. 10A), where increased density of F4/80-expressing cells was apparent in all grafts from all time points compared to the normal mouse skin. Quantification of the macrophage number in xenografts revealed that within the first month, the xenografts with the deep dermal scratch wounds performed before or after grafting had higher macrophages than the nonscratch wound grafts (3.8 ± 0.5 and 4.1 ± 0.4 vs. 2.3 ± 0.3 mean fold change, respectively $p < 0.05$). At 2 months after grafting, macrophages showed the highest number in all groups; however, there was no significant difference between them. At 3 months after grafting, macrophages in the scratch wound xenografts whether before or after transplantation were higher than the nonscratch wound xenografts (3.4 ± 0.22 and 3.4 ± 0.5 vs. 2.0 ± 0.2 mean fold change, respectively $p < 0.05$) (Fig. 10B). This suggests a persistent inflammatory response caused by the deep dermal scratch wound, which was a feature fibroproliferative disorder, such as human HTS.[2,5]

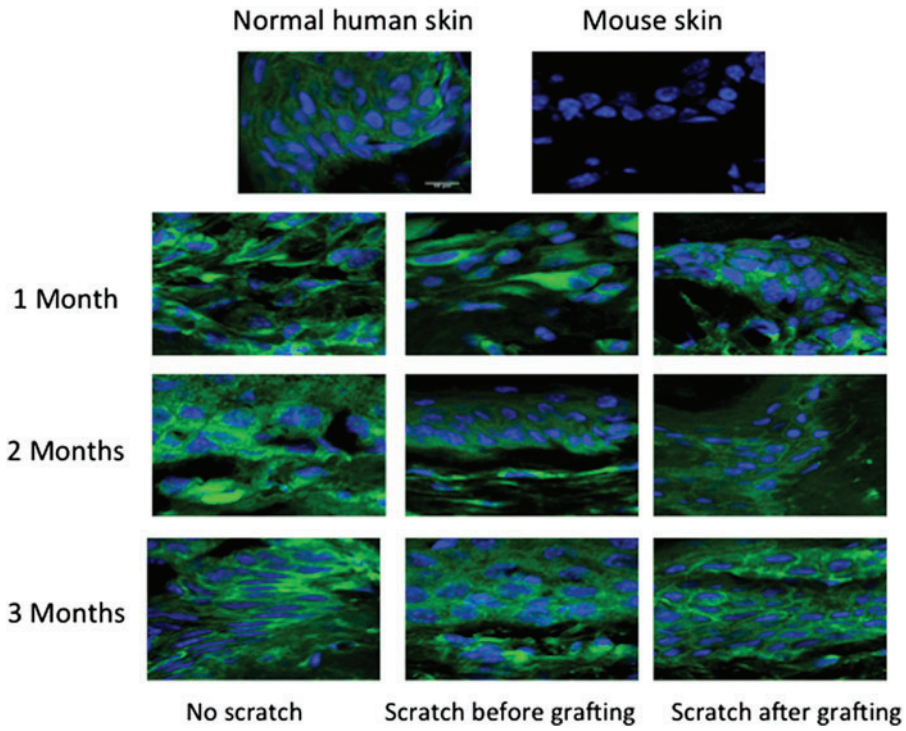

Figure 9. Representative images of anti-human FITC human leukocyte antigen-ABC antibody stained sections confirm survival of transplanted human xenografts at all time points. Showing positive staining with *green,* net-like, immunofluorescent staining pattern that is consistent with normal human skin compared to normal mouse skin, which has no visible green staining (negative control). To see this illustration in color, the reader is referred to the web version of this article at www.liebertpub.com/wound

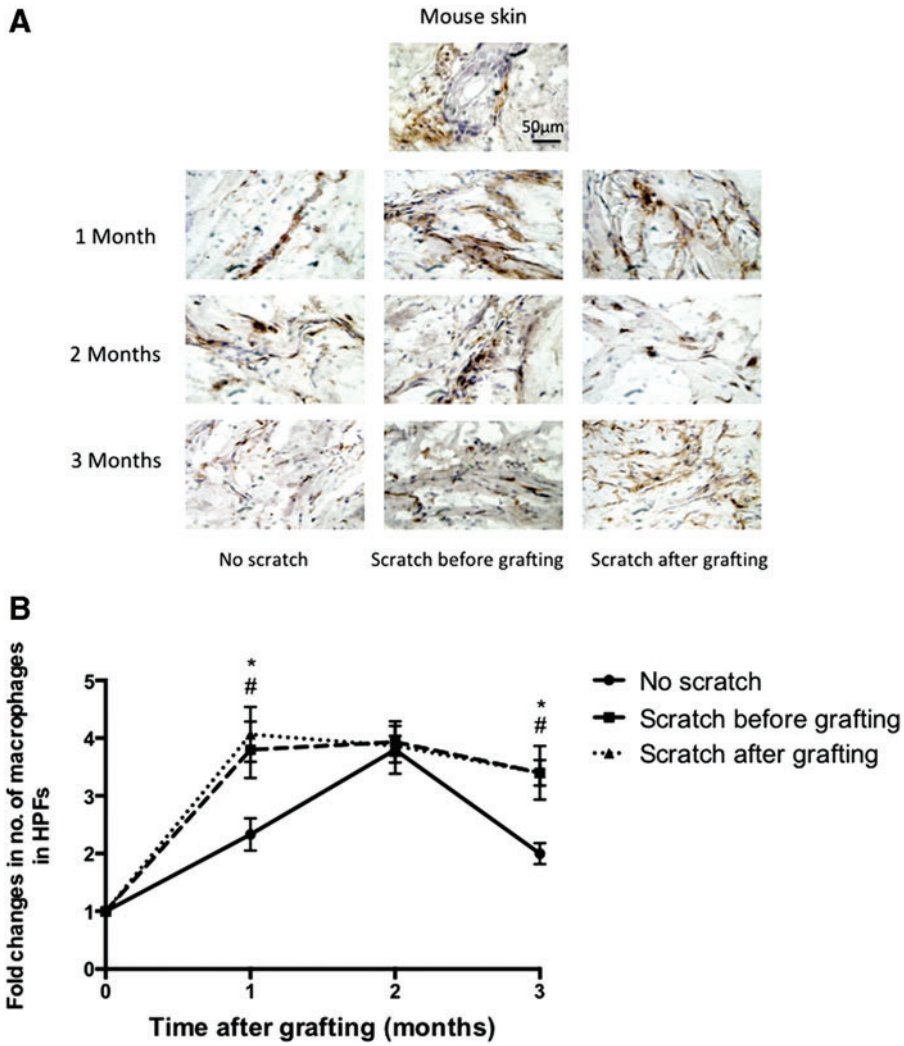

Figure 10. **(A)** Immunohistochemistry staining using an anti-F4/80 antibody showing macrophages in normal mouse skin and transplanted xenografts in all time points. Scale bar = 50 μm. **(B)** Fold changes in macrophages, measured in five randomly selected site/field. No scratch grafts (*circle*), scratch before grafting (*square*), and scratch after grafting (*triangle*). $^{\#}p < 0.05$ compared between the scratch before grafting and no scratch group in the same time point. $^{*}p < 0.05$ compared between the scratch after grafting and no scratch group in the same time ($n = 4$). To see this illustration in color, the reader is referred to the web version of this article at www.liebertpub.com/wound

Mast cells in the human skin xenografts

Increased mast cell density has been reported in human HTS[22] as well as in animal models of HTS,[18,19] which has been suggested to account for the pruritus and pain in fibrotic tissues associated with mast cell degranulation.[23] Using toluidine blue staining, mast cells were significantly increased in xenografts at all time points (Fig. 11A) compared to the normal human skin. Mast cells peaked at 2 months, then significantly decreased at 3 months for all the groups. The mast cell mean fold changes for the nonscratch group were 2.2 ± 0.4, 3.5 ± 0.17, and 1.55 ± 0.34, respectively, after 1, 2, and 3 months compared to the scratch before the grafting group with the deep dermal scratch performed before transplantation (2.4 ± 0.5 and 3.2 ± 0.23 and 1.6 ± 0.13) and the deep dermal scratch after transplantation (3.3 ± 0.17 and 4.5 ± 0.11 and 2.05 ± 0.52). However, there was no significant difference in the mast cells between the scratch wound grafts, whether before or after grafting, and the nonscratched grafts in all time points (Fig. 11B).

DISCUSSION

Despite considerable research in skin wound healing, the pathogenesis of dermal fibrosis is still poorly understood.[3] The lack of an ideal animal model representative of human dermal fibrosis limits our understanding on the underlying mechanisms of fibrosis and hinders the accuracy and applicability in testing the effectiveness and safety

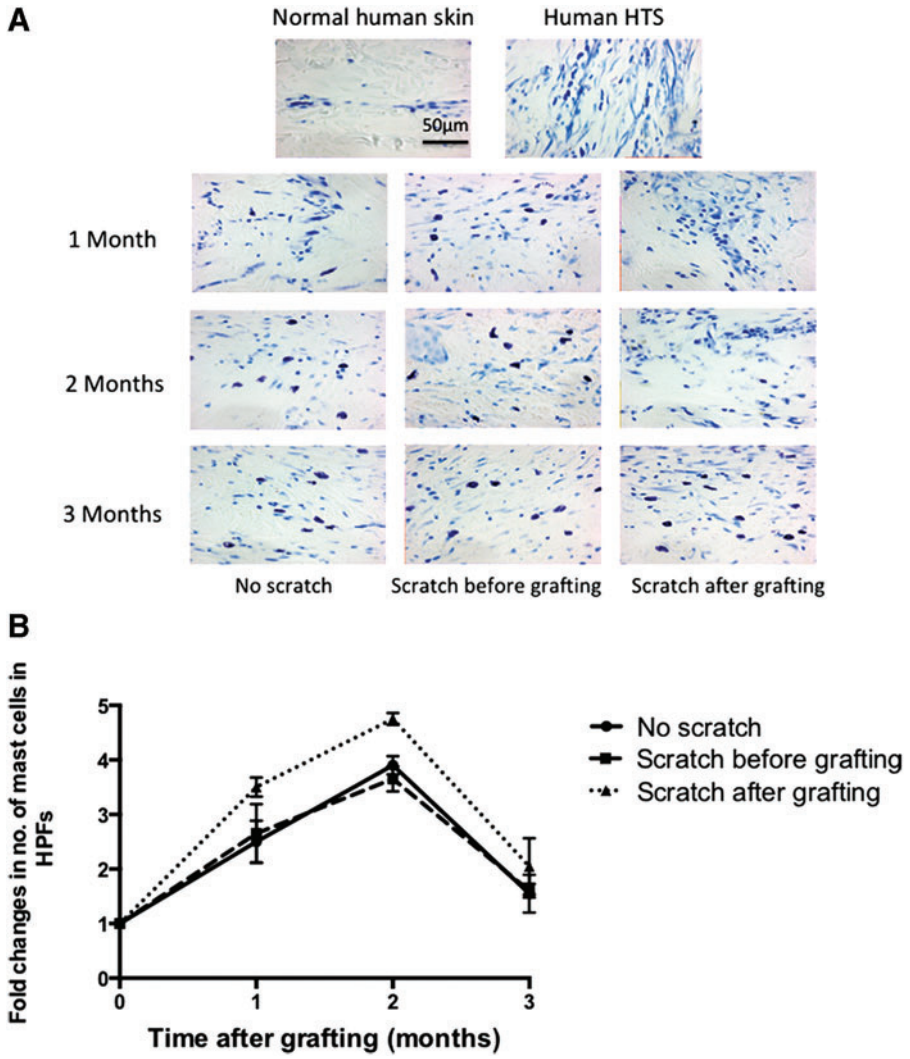

Figure 11. **(A)** Representative images of a toluidine blue stained section of human normal skin, HTS, and transplanted xenografts at all time points showing an increased density red purple staining of mast cells similar to human HTS compared to fewer mast cells seen in normal human skin. Scale bar = 50 μm. **(B)** Fold changes in mast cells, measured in five randomly selected site/field. No scratch grafts (*circle*), scratch before grafting (*square*), and scratch after grafting (*triangle*). To see this illustration in color, the reader is referred to the web version of this article at www.liebertpub.com/wound

of novel antifibrotic therapies. Unfortunately, HTS develops only in human and not animal skin, which makes the reliability of therapies effective in animal tissues using commonly used models of scarring to date such as the rabbit ear[15] or the dorsum of the red Duroc pig, of questionable translational value for human fibroproliferative disorders.[24]

Various reports attempt to describe the animal models of HTS, including the rabbit ear model,[15] by making a deep incision overlying the ear cartilage of the rabbit that developed inflamed and hypertrophied scar. The ability of making many scars in each ear and using multiple treatments are the main advantages of this model.[25,26] The wound environment in this model is different from that of the dermal fibrosis, in which the ear cartilage, as well as the dermis, undergoes hypertrophy, which contributes to scar thickness but is not truly representative of dermal scarring in humans where perichondral hypertrophy is not present in the scar that humans develop.

Because pig skin has been found to more closely resemble human tissues in terms of the lack of contraction due to an absence of panniculus carnosus and the dependence on external sources of Vitamin C to support collagen metabolism, the female red Duroc pig has been used to develop a HTS-like model by making deep wounds onto the back of the animal, which results in a thick scar.[24] However, this scar is not erythematous and raised, typical features of human HTS, but instead depressed, making it morphologically dissimilar to human HTS in addition to being an expensive and more difficult to handle model, which limits its use.

Recently, the use of subcutaneous osmotic pumps in nude mice delivering bleomycin has resulted in the development of a fibrotic scar over the back of the animals,[27] which has some features similar to human HTS. However, the need for continuous delivery of bleomycin for the development of fibrosis, which resolves quickly after discontinuing the drug, makes the model worthy of consideration but the tissues affected are murine, the morphologic features differ significantly from human HTS, and the testing of antifibrotic therapies will be complicated and difficult in this model.

The athymic nude mouse model was established by Yang *et al.*[28] by transplanting full thickness human skin onto the back of the mice. This procedure developed a graft that had features similar to that of human HTS. This model has been modified more by transplanting a split thickness skin graft that also developed similar characteristics of human HTS.[18,19] Because HTS occurs after injury to a critical depth in the dermis of human skin,[12] we attempted to test the deep dermal scratch model validated in humans to develop a reproducible typical HTS to the skin when the injury exceeds 0.56 mm in depth in the dermis, to similarly injured human skin either before or after transplantation onto the athymic nude mouse. Deep dermal injury to the human skin either before or after transplantation successfully engrafts and subsequently developed thickened raised scars, which persisted beyond 1 year. Reepithelialization occurs by migration of adjacent human epithelial cells in the engrafted human skin similar to human skin injuries.[29] The raised thickened dermal scar that develops after deep dermal injury in the transplanted human skin contains substantial number of fibroblasts, mast cells, myofibroblasts, and macrophages very typical of human HTS,[30] and while some of these cells stained for human ABC antigen in the skin, others may arise from the bone marrow of the mouse, which is yet to be conclusively determined.

In the past, bone marrow-derived cells such as fibrocytes, macrophages, and mast cells have been confirmed to be present in the healing human skin engrafted on the nude mice, which likely play an important regulatory role in scar formation.[31] While many of these immunologic cells are likely derived from the mouse, murine immunology is well characterized compared to other animal species and resembles human immune responses, which further adds to the unique features of the model that are similar to human responses to injury.[30]

Prolonged inflammation is highly associated with dermal scarring.[30] Inflammatory cells infiltration is essential for wound repair; however, increased amounts and activity of the macrophage, especially in the maturation phase, could cause an increase in ECM deposition and lead to fibrotic scar.[32] In this study, increased macrophage infiltration was observed in all the grafts compared to normal skin, which is consistent to our previous observation.[19] However, scratching the grafts before and after transplanting induced more macrophage infiltration to the grafts that were significantly observed at 3 months, indicating prolonged inflammation where the increased numbers of macrophages likely lead to increased ECM deposition through paracrine cytokine production similar to human HTS.[33] The macrophage is an important immune cell in wound healing. It has multiple functions during skin repair, including phagocytosis, antigen presenting, and cytokine and chemokine production, which promote angiogenesis, fibroblast proliferation, and collagen synthesis.[34] It is a key cell that coordinates the wound healing process throughout the multiple phases.[32,35] It has been found that mice genetically engineered to produce nonfunctional macrophages at different stages of healing have inadequate wound repair due to a delay in reepithelialization and neovascularization in addition to improper granulation tissue formation after depletion of macrophages during the inflammatory phase of wound healing.[35,36] Depletion of macrophages during the maturation phase did not show any significant delay in wound repair.[37] However, alternative techniques exist for timely depletion of macrophages such that the role of macrophage function during different phases of scar formation after deep dermal injury to the human skin transplanted onto athymic mice as described herein will be helpful to understand more their effects in HTS formation as well as to test novel drugs targeting macrophages.

Other bone marrow-derived cells that are important in fibrotic disorders include mast cells, which were increased significantly in all three types of xenografts by 2 months post-transplantation compared to normal skin. However, there was no significant difference among the scratched and nonscratched grafts at all time points. Mast cells have several roles in wound healing. They release many mediators from their granules after being stimulated by skin injury.[23] They promote inflammation, reepithelialization, and increased vascular permeability and angiogenesis.[38] Moreover, histamine increases fibroblast proliferation and its differentiation into the contractile myofibroblast.[39] Several studies have shown mast cell involvement in scar formation by affecting collagen maturation and remodeling[40,41] Although increased mast cell num-

ber and activity occurs in HTS,[42] lower mast cell numbers have been found in scarless regenerative wound healings such as fetal wounds and oral mucosal wounds.[43,44] It has been reported that wounds in mast cell-deficient mice heal with minimal scar tissue compared to the wild type, suggesting that a significant role of mast cells exists during fibrotic scar formation in this model.[43,45]

An important unique feature of the deep dermal scratch in this model is the significantly increased number of α-SMA–expressing myofibroblasts observed at 2 months post-transplantation compared to the intact human skin without the deep dermal injury. This finding correlates with the increase in wound contraction and reduced graft area observed compared to the nonscratched model. The increase in scar thickness also suggests an increase in the synthesis and deposition of ECM.[46] Myofibroblasts have an important role in wound healing by inducing wound closure, collagen secretion, and reorganizing ECM.[47] They may originate from several cell types, such as pericytes, chondrocytes, osteoblasts, and circulating fibrocytes; however, most appear to arise from local connective tissue fibroblasts.[48] The differentiation of myofibroblasts from the local fibroblast is likely induced by the TGF-β1, which has been reported to increase the expression of myofibroblasts; whereas, reduction in TGF-β inducible early gene (TIEG) knockout mice decreases both wound contraction and myofibroblast infiltration in tissues supporting the importance of TGF-β1 for myofibroblast differentiation, wound contraction, and fibrotic matrix accumulation.[49] Previously, we have described increased bone marrow-derived fibrocytes in the transplanted human skin in the nude mouse model, which can be an additional source of TGF-β for indirect stimulation of myofibroblast differentiation,[19] or also directly forming the myofibroblastic phenotype from fibrocytes recruited to the site of tissue injury.[50] In normal wound healing, the myofibroblasts undergo apoptosis and disappear from the granulation tissue after wound closure; however, in HTS, these cells fail to undergo apoptosis and continue to be present in the fibrotic tissue similar to our findings. This persistent expression of α-SMA myofibroblasts in all the time points in the mouse model is a consistent feature of human HTS.[51]

Thus, the presence of increased numbers of bone marrow-derived macrophages, mast cells, and fibrocytes associated with the increase in dermal fibrosis in the deep dermal scratch model suggests that an important role exists for systemically derived cells in the fibrosis in human skin. This is in addition to the local activation of unique HTS-like fibroblasts present in the deep dermis, which we have previously shown to very closely resemble the fibroblasts found in HTS compared to fibroblasts found in the upper layers of the dermis or in site-matched normal skin.[13,14] Bone marrow-derived cells appear to be contributed to the injured tissue in this model and they may promote angiogenesis and cytokine and chemokine production, and ECM deposition as described in other models of wound healing.[52,53] In the future, this model may permit ongoing investigation into the relative importance of locally derived fibroblasts versus bone marrow-derived cells in human fibrosis so that more effective antifibrotic strategies can be developed.[53] The deep dermal scratch will facilitate topical application of antifibrotic agents to determine the effectiveness of local versus systemic antifibrotic therapies. The creation of the deep dermal scratch in the human skin performed before transplantation results in fibrosis very similar to that, which occurs following deep dermal scratch after the human skin has been successfully grafted. This will increase the usefulness of the model, where the deep dermal scratch created *ex vivo* before transplantation is much easier to perform, safer than injuring the mice *in vivo*, and avoids the need to burn or create other injuries to the animals *in vivo*, thereby minimizing the suffering of animals used to study human fibrotic disorders.

In conclusion, we observed that human skin grafts transplanted to athymic mice with a deep dermal injury, created either *ex vivo* or *in vivo*, developed a thickened contracted fibrotic scar with similar morphologic and histologic features of human HTS. In addition, human cellular elements are retained in the fibrotic tissues for at least 1 year after transplantation. Compared to the nonscratched

KEY FINDINGS

- We compared the fibrotic scar formation in athymic mice in relation to deep dermal injury of the grafted human skin created before or after transplanting it and without deep dermal injury.
- Deep dermal injury to human skin grafts transplanted to athymic mice made either before or after transplantation developed similar morphologic and histologic features of human HTS.
- Human cellular elements are retained in the scratched xenografts for 1 year after transplantation.
- This model would aid the researches of both local topical and systemic novel antifibrotic therapies.

model of human skin on the transplanted in the athymic model previously described,[19] the deep dermal injury had increased wound contraction, scar thickness and fibrosis, and prolonged inflammatory cell infiltration, including macrophages, mast cells, and α-SMA–expressing myofibroblasts.

INNOVATION

The deep dermal injury in the transplanted human skin either before or after transplantation led to very similar degrees of fibrosis, creating deep dermal injury to human skin *ex vivo* before transplantation will afford a representative, affordable, ethical, and practical model for studying the local and systemic factors involved in scarring in human skin tissues in the future. The fibrosis, which develops and persists in human skin in this animal model will also facilitate the investigation of both local topical and systemic novel antifibrotic therapies with likely improved translational effectiveness in human dermal fibrotic conditions, including HTS.

ACKNOWLEDGMENTS AND FUNDING SOURCES

The authors gratefully acknowledge the support for this study from the Firefighters' Burn Trust Fund of the University of Alberta, the Edmonton Civic Employees Research Fund, and King Fahad Specialist Hospital-Dammam, Saudi Arabia.

AUTHOR DISCLOSURE AND GHOSTWRITING

None of the authors has any financial interest in the products, devices, or drugs mentioned in this article. The authors listed wrote this article. No ghostwriters were used to write this article.

ABOUT THE AUTHORS

Saad M. Alrobaiea, MD, is a graduate student for Master Degree. **Jie Ding, PhD,** is a research associate, and supervisor of the student. **Zengshuan Ma, PhD,** is a laboratory technician. **Edward E. Tredget, MD, MSc,** is a full professor, and supervisor of the student.

REFERENCES

1. Schilling JA. Wound healing. Surg Clin North Am 1976;56:859–874.
2. Reinke JM, Sorg H. Wound repair and regeneration. Eur Surg Res 2012;49:35–43.
3. Broughton G II, Janis JE, Attinger CE. The basic science of wound healing. Plast Reconstr Surg 2006;117(7 Suppl):12S–34S.
4. Deitch EA, Wheelahan TM, Rose MP, et al. Hypertrophic burn scars: analysis of variables. J Trauma 1983;23:895–898.
5. Tredget EE. Pathophysiology and treatment of fibroproliferative disorders following thermal injury. Ann N Y Acad Sci 1999;888:165–182.
6. Nedelec B, Ghahary A, Scott PG, et al. Control of wound contraction. Basic and clinical features. Hand Clin 2000;16:289–302.
7. Wynn TA. Cellular and molecular mechanisms of fibrosis. J Pathol 2008;214:199–210.
8. Armour A, Scott PG, Tredget EE. Cellular and molecular pathology of HTS: basis for treatment. Wound Repair Regen 2007;15 Suppl 1:S6–S17.
9. Brissett AE, Sherris DA. Scar contractures, hypertrophic scars, and keloids. Facial Plast Surg 2001;17:263–272.
10. Ogawa R, Chin MS. Animal models of keloids and hypertrophic scars. J Burn Care Res 2008;29: 1016–1017.
11. Ramos MLC, Gragnani A, Ferreira LM. Is there an ideal animal model to study hypertrophic scarring? J Burn Care Res 2008;29:363–368.
12. Dunkin CSJ, Pleat JM, Gillespie PH, et al. Scarring occurs at a critical depth of skin injury: precise measurement in a graduated dermal scratch in human volunteers. Plast Reconstr Surg 2007;119: 1722–1732.
13. Honardoust D, Varkey M, Marcoux Y, et al. Reduced decorin, fibromodulin, and transforming growth factor-β3 in deep dermis leads to hypertrophic scarring. J Burn Care Res 2012;33:218–227.
14. Honardoust D, Ding J, Varkey M, et al. Deep dermal fibroblasts refractory to migration and decorin-induced apoptosis contribute to hypertrophic scarring. J Burn Care Res 2012;33:668–677.
15. Morris DE, Wu L, Zhao LL, et al. Acute and chronic animal models for excessive dermal scarring: quantitative studies. Plast Reconstr Surg 2012;100:674–681.
16. Zhu KQ, Engrav LH, Gibran NS, et al. The female, red Duroc pig as an animal model of hypertrophic scarring and the potential role of the cones of skin. Burns Incl Therm Inj 2003;29:649–664.
17. Seo BF, Lee JY, Jung S-N. Models of abnormal scarring. Biomed Res Int 2013;2013:1–8.
18. Momtazi M, Kwan P, Ding J, et al. A nude mouse model of hypertrophic scar shows morphologic and histologic characteristics of human hypertrophic scar. Wound Repair Regen 2013;21:77–87.
19. Wang J, Ding J, Jiao H, et al. Human hypertrophic scar-like nude mouse model: Characterization of the molecular and cellular biology of the scar process. Wound Repair Regen 2011;19:274–285.
20. Ding J, Ma Z, Liu H, et al. The therapeutic potential of a C-X-C chemokine receptor type 4 (CXCR-4) antagonist on hypertrophic scarring *in vivo*. Wound Repair Regen 2014;22:622–630.
21. Junqueira LC, Cossermelli W, Brentani R. Differential staining of collagens type I, II and III by Sirius Red and polarization microscopy. Arch Histol Jpn 1978;41:267–274.
22. Tredget EE, Shankowsky HA, Pannu R, et al. Transforming growth factor-beta in thermally injured patients with hypertrophic scars: effects of interferon alpha-2b. Plast Reconstr Surg 1998;102:1317–1328; discussion 1329–1330.
23. Wulff BC, Wilgus TA. Mast cell activity in the healing wound: more than meets the eye? Exp Dermatol 2013;22:507–510.
24. Gallant CL, Olson ME, Hart DA. Molecular, histologic, and gross phenotype of skin wound healing in red Duroc pigs reveals an abnormal healing phenotype of hypercontracted, hyperpigmented scarring. Wound Repair Regen 2004;12:305–319.
25. Ko JH, Kim PS, Zhao Y, et al. HMG-CoA reductase inhibitors (statins) reduce hypertrophic scar formation in a rabbit ear wounding model. Plast Reconstr Surg 2012;129:252e–261e.
26. Reid RR, Mogford JE, Butt R, et al. Inhibition of procollagen C-proteinase reduces scar hypertrophy in a rabbit model of cutaneous scarring. Wound Repair Regen 2006;14:138–141.
27. Cameron AM, Adams DH, Greenwood JE, et al. A novel murine model of hypertrophic scarring using

subcutaneous infusion of bleomycin. Plast Reconstr Surg 2014;133:69–78.

28. Yang DY, Li SR, Wu JL, et al. Establishment of a hypertrophic scar model by transplanting full-thickness human skin grafts onto the backs of nude mice. Plast Reconstr Surg 2007;119:104–109; discussion 110–111.
29. Ud-Din S, Volk SW, Bayat A. Regenerative healing, scar-free healing and scar formation across the species: current concepts and future perspectives. Exp Dermatol 2014;23:615–619.
30. Lupher ML Jr., Gallatin WM. Regulation of fibrosis by the immune system. Adv Immunol 89;2006:245–288.
31. Wang JF, Jiao H, Stewart TL, et al. Fibrocytes from burn patients regulate the activities of fibroblasts. Wound Repair Regen 2007;15:113–121.
32. Delavary BM, van der Veer WM, van Egmond M, et al. Macrophages in skin injury and repair. Immunobiology 2011;216:753–762.
33. Kendall RT, Feghali-Bostwick CA. Fibroblasts in fibrosis: novel roles and mediators. Front Pharmacol 2014;5:123.
34. Park JE, Barbul A. Understanding the role of immune regulation in wound healing. Am J Surg 2004;187:S11–S16.
35. Leibovich SJ, Ross R. The role of the macrophage in wound repair. A study with hydrocortisone and antimacrophage serum. Am J Pathol 1975;78:71–100.
36. Mirza R, Dipietro LA, Koh TJ. Selective and specific macrophage ablation is detrimental to wound healing in mice. Am J Pathol 2010;175:2454–2462.
37. Lucas T, Waisman A, Ranjan R, et al. Differential roles of macrophages in diverse phases of skin repair. J Immunol 2010;184:3964–3977.
38. Wilgus TA, Wulff BC. The importance of mast cells in dermal scarring. Adv Wound Care 2014;3:356–365.
39. Gailit J, Marchese MJ, Kew RR, et al. The differentiation and function of myofibroblasts is regulated by mast cell mediators. J Invest Dermatol 2001;117:1113–1119.
40. Younan GJ, Heit YI, Dastouri P, et al. Mast cells are required in the proliferation and remodeling phases of microdeformational wound therapy. Plast Reconstr Surg 2011;128:649e–658e.
41. Iba Y, Shibata A, Kato M, et al. Possible involvement of mast cells in collagen remodeling in the late phase of cutaneous wound healing in mice. Int Immunopharmacol 2004;4:1873–1880.
42. Kischer CW, Bunce H, Shetlah MR. Mast cell analyses in hypertrophic scars, hypertrophic scars treated with pressure and mature scars. J Invest Dermatol 1978;70:355–357.
43. Wulff BC, Parent AE, Meleski MA, et al. Mast cells contribute to scar formation during fetal wound healing. J Invest Dermatol 2012;132:458–465.
44. Szpaderska AM, Zuckerman JD, DiPietro LA. Differential injury responses in oral mucosal and cutaneous wounds. J Dent Res 2003;82:621–626.
45. Shiota N, Nishikori Y, Kakizoe E, et al. Pathophysiological role of skin mast cells in wound healing after scald injury: study with mast cell-deficient W/W(V) mice. Int Arch Allergy Immunol 2010;151:80–88.
46. Hinz B. The myofibroblast: Paradigm for a mechanically active cell. J Biomech 2010;43:146–155.
47. Tomasek JJ, Gabbiani G, Hinz B, et al. Myofibroblasts and mechano-regulation of connective tissue remodelling. Nat Rev Mol Cell Biol 2002;3:349–363.
48. Hinz B, Phan SH, Thannickal VJ, et al. The myofibroblast: one function, multiple origins. Am J Pathol 2007;170:1807–1816.
49. Hori K, Ding J, Marcoux Y, et al. Impaired cutaneous wound healing in transforming growth factor-β inducible early gene1 knockout mice. Wound Repair Regen 2012;20:166–177.
50. Abe R, Donnelly SC, Peng T, et al. Peripheral blood fibrocytes: differentiation pathway and migration to wound sites. J Immunol 2001;166:7556–7562.
51. Linge C, Richardson J, Vigor C, et al. Hypertrophic scar cells fail to undergo a form of apoptosis specific to contractile collagen-the role of tissue transglutaminase. J Invest Dermatol 2005;125:72–82.
52. Bucala R, Spiegel LA, Chesney J, et al. Circulating fibrocytes define a new leukocyte subpopulation that mediates tissue repair. Mol Med 1994;1:71–81.
53. Quan TE, Cowper SE, Bucala R. The role of circulating fibrocytes in fibrosis. Curr Rheumatol Rep 2006;8:145–150.

Abbreviations and Acronyms

α-SMA = α-smooth muscle actin
BSA = bovine serum albumin
DAB = 3, 3′-diaminobenzidine
ECM = extracellular matrix
FPD = fibroproliferative disease
H&E = hematoxylin and eosin
HLA = human leukocyte antigen
HTS = hypertrophic scar
IgG = immunoglobulin G
TGF-β = transforming growth factor-β
TIEG = TGF-β inducible early gene